Spin transport in carbon nanotubes with magnetic vacancy-defects

Zeila Zanolli and J.-C. Charlier
Institute of Condensed Matter and Nanosciences–Nanophysics (IMCN/NAPS), European Theoretical Spectroscopy Facility (ETSF), Université catholique de Louvain, Place Croix du Sud 1 (Boltzmann), 1348 Louvain-la-Neuve, Belgium
(Received 11 January 2010; revised manuscript received 5 March 2010; published 2 April 2010)

The spin-polarized electron transport properties of metallic carbon nanotubes containing vacancies are investigated using first-principles and nonequilibrium Green's function techniques. Reconstructed mono- and trivacancies, containing carbon atoms with unsaturated bonds, behave like quasilocalized magnetic impurities. However, in conventional *ab initio* simulations, these magnetic defects are artificially repeated periodically (supercell method) and are thus incorrectly coupled by long range interactions. Consequently, a technique based on an open system with an isolated magnetic impurity is used here to accurately describe the local magnetic properties of these defects, revealing spin-dependent conductances in tubes, which could be exploited in spintronic nanodevices.

DOI: 10.1103/PhysRevB.81.165406 PACS number(s): 61.46.Fg, 71.15.Mb, 73.22.−f, 73.63.Fg

I. INTRODUCTION

Carbon nanotubes (CNTs) (Ref. 1) are one-dimensional (1D) nanostructured materials renowned in the scientific community for being both a playground for studying fundamental physical properties[2,3] and for numerous potential applications in electronics,[4] and spintronics.[5] Due to the weak spin-orbit and hyperfine interactions in carbon-based materials, the coherence length for spin propagation in CNTs is quite long (0.13–1.4 μm at 4.2 K).[6] This, together with the ballistic nature of electron conduction[7] in CNTs, makes the latter exceptional candidates for quantum transport devices and spintronic applications.

However, despite the progresses in growth techniques,[8] CNTs always present structural defects[9] and their electronic and transport properties are affected accordingly.[10] In addition, the presence of defects in carbon-based nanostructures has been seen as a source of magnetism.[11] Consequently, mastering the physics underlying defected CNTs is crucial not only to model realistic systems but also to tune the tube properties in a desired direction in order to design new devices.

Ab initio ground-state spin polarized studies of CNTs with mono- and divacancies have been reported in,[12–15] but the exact value of the magnetization of point defected tubes is still debated and found to be dependent on the number of cells used in the calculation.[16] In fact, the goal of the present work consists in demonstrating that this issue is intrinsic to the periodic boundary conditions (PBC) scheme traditionally employed to treat the defected CNT system using the supercell technique. Indeed, the interaction among the periodic replicas of the magnetic impurity can affect the computed magnetic properties, even for very long supercells. Consequently, a nonperiodic system has to be used to study the magnetic properties of a CNT with a single defect site. Within this approach spurious interactions are avoided and it can definitively be assessed that carbon atoms with unsaturated bonds, such as in mono- and trivacancies, act as magnetic impurities for CNTs.

II. COMPUTATIONAL METHODS

In this work, spin-polarized first-principles density functional theory (DFT) (Ref. 17) calculations for metallic (5,5) CNTs with mono-, di-, and trivacancies are presented. The magnetic properties are investigated both by the traditional PBC scheme and by a nonperiodic open-system scheme. The latter method is actually essential to accurately assess the magnetic properties of such nanosystems. The spin-polarized electron transmission functions are then calculated within the nonequilibrium Green's function (NEGF) formalism, using the one-particle Hamiltonian obtained from the DFT calculations.[18] The defective (10,10) tube has also been studied to allow a comparison with previous spin-polarized calculations,[15] where the reconstructed monovacancy was found to be nonmagnetic. This inconsistency with our work is suggested to be a consequence of the technical details of the calculations described in Ref. 14. Our calculations definitely demonstrate that a finite magnetization is observed and predicted numerically whenever an unsaturated carbon bond is present.

Conventional periodic boundary conditions calculations are performed within the local spin density approximation, using norm-conserving pseudopotentials[19] and numerical atomic orbital basis sets of double-ζ quality with one polarization orbital (DZP).[20] The real-space grid cutoff is 300 Ry and a Fermi-Dirac distribution function with an electronic temperature of 10 meV is used to populate the energy levels. To investigate the dependence of the magnetization from the distance between the defects, $1\times1\times n$ supercells with n ranging from 5 to 15 are considered. The geometry is fully relaxed until the forces on each atom and on the unit cell are less than 0.01 and 0.03 eV/Å, respectively. The lateral dimension of the cell was fixed to ensure an intertube distance larger than 13Å. The integration over the 1D Brillouin zone is replaced by a summation over a regular grid of k-points with a k-point spacing equivalent to $\sim$180 k-points for the armchair unit cell.

III. RESULTS AND DISCUSSION

A. Structural properties

Within such a framework, various geometrical reconstructions of vacancy-defected CNTs are studied. By removing

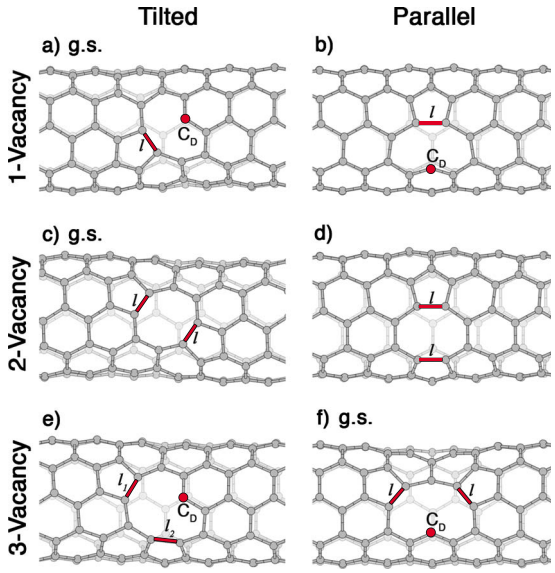

FIG. 1. (Color online) Ball-and-stick models illustrating fully *ab initio* optimized atomic structures of a (5,5) CNT containing a reconstructed monovacancy (a, b), divacancy (c, d), and trivacancy (e, f) in various topological orientations (*tilted* and *parallel*, as defined in the text). The most stable structure for each defect type is labeled as ground state (*g.s.*). The newly formed carbon bonds (red sticks) and the dangling carbon atoms (red balls) are indicated by l and C_D, respectively.

one C atom from the hexagonal net, three C atoms are left with an unsaturated bond. When the system is relaxed, the monovacancy undergoes a Jahn-Teller distortion: two of the unsaturated carbon atoms form a weak covalent bond resulting in a pentagonal rearrangement. This new bond is indicated by l in Fig. 1(a) (most stable structure or ground-state configuration, with a corresponding total energy $E_{g.s.}$) and Fig. 1(b) (next stable structure, i.e., the closest configuration to the ground-state one, exhibiting a total energy $E' > E_{g.s.}$).[21] The third unsaturated carbon atom [labeled C_D in Fig. 1(a) and Fig. 1(b)] moves radially out of the tube modifying the initial D_{3h} symmetry of the hexagonal network into the favored C_s symmetry.[22] For each defect type, bond lengths of the reconstructed structures and total energy differences ($\Delta E = E' - E_{g.s.}$) between the two most stable configurations are collected in Table I.

Similarly, the trivacancy reconstructs into two pentagons and one decagon,[23] leaving one carbon atom unsaturated, as illustrated in Fig. 1(e) (next stable structure) and Fig. 1(f) (ground state). The two possible orientations of reconstructed vacancies are here referred to as *tilted* or *parallel* as function of whether the C_D atom belongs to a tilted or parallel zigzag profile with respect to the tube axis. On the other hand, the di-vacancy reconstructs into two pentagons and one octagon[10] without any unsaturated carbon atom. In this case, *tilted* and *parallel* refer to the direction of the newly formed bond of the pentagons, denoted by l in Fig. 1(c) (ground state) and Fig. 1(d) (next stable structure). Despite the energetic ordering of the reconstructed structures may depend on the tube curvature,[23] the ground-state configuration is the tilted for the mono- and divacancy, and the parallel for the trivacancy in agreement with previously published results.[10,21,23] Indeed, since the tube diameter can shrink to accommodate new shorter bonds formed in the direction perpendicular to the tube axis, the structures with the maximum numbers of such bonds are the most stable ones for each type of defect.

B. Magnetic properties and the indirect exchange coupling

Since the localized orbitals of unsaturated carbon atoms are expected to behave as magnetic impurities,[11] a net magnetic moment is expected for both mono- and trivacancies and no magnetism for divacancies. However, PBC calculations can lead to results in contradiction with these predictions. For instance, the total magnetic moment of the tilted divacancy computed using the $1 \times 1 \times 15$ supercell is $\sim 0.013\ \mu_B$, and a magnetic moment of $\sim 0.5\ \mu_B$ has been reported in[14] for the parallel divacancy in the (6, 6) nanotube. Interestingly, the total magnetic moment of CNTs containing the tilted monovacancy oscillates with the length nd_0 of the $1 \times 1 \times n$ supercell (d_0 being the length of the (5,5) unit cell) and finally goes to zero as illustrated in Fig. 2 (square marks). It is worth notice that these oscillations are not due to a poor k-point sampling of the Brillouin zone since accurate convergence studies have been performed. For instance, the magnetic moment of the $1 \times 1 \times 12$ supercell of the tilted monovacancy changes only by $0.010\ \mu_B$ when the sampling of the 1D Brillouin zone is increased from 18 to 254 k-points.

In fact, these oscillations of the total magnetic moment are due to a long range interaction between the periodic images of the magnetic moments mediated by the conduction electrons of the metallic tube, also called indirect exchange

TABLE I. Total energy difference $\Delta E = E' - E_{g.s.}$ (eV) between the most ($E_{g.s.}$) and the next (E') stable reconstructed structures of (5,5) CNT with a mono-, di-, or trivacancy, respectively. Bond lengths (Å) of the dangling carbon (C_D) and between the two carbon forming the pentagons (l) for each structure, as illustrated in Fig. 1.

		Tilted		Parallel	
	ΔE	C_D	l	C_D	l
1 vacancy	1.343	1.39	1.54	1.37	1.64
2 vacancy	1.850		1.49		1.54
3 vacancy	0.980	1.39	1.50(l_1) 1.59(l_2)	1.38	1.51

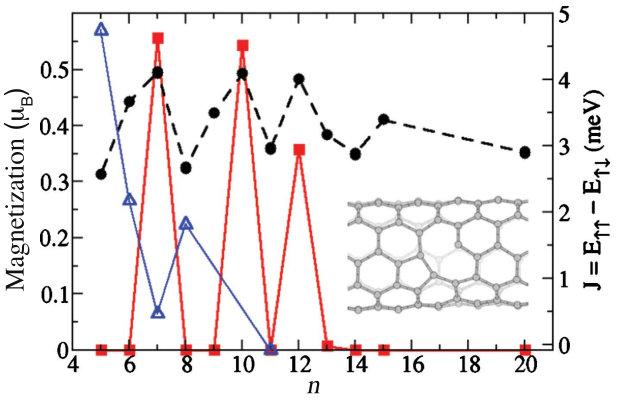

FIG. 2. (Color online) Total magnetization (μ_B) for the $1\times1\times n$ supercell containing one monovacancy calculated within the PBC scheme (red curve ■—■) and for the open system with $1\times1\times n$ *core* region (black curve ●—●). Indirect Exchange coupling (J, meV) for the $1\times1\times2n$ supercell containing two monovacancies at distance nd_0 (blue curve ▲—▲). All the calculations are performed on a (5,5) CNT containing a monovacancy reconstructed in the tilted configuration, as illustrated in the inset.

coupling.[24] This indirect coupling is defined as the energy required to rotate the magnetic moments from the ferromagnetic to the antiferromagnetic configuration, that is $J=E_{\uparrow\uparrow}-E_{\uparrow\downarrow}$, where $E_{\uparrow\uparrow}$ and $E_{\uparrow\downarrow}$ are the total energies of the ferromagnetic and antiferromagnetic configurations, respectively. The interaction results in an oscillatory behavior of J whose amplitude decreases as a power law of the distance between the magnetic impurities. Such a power law strongly depends on the nature of the impurity and on the dimensionality of the system. When the supercell contains a single defect, PBCs allow exclusively either a non-spin-polarized configuration or a ferromagnetic coupling between the periodically repeated magnetic impurities. Hence, when their distance is such that the antiferromagnetic coupling is the lowest-energy configuration (i.e., $J>0$), the periodic system is forced into either a non-spin-polarized or a ferromagnetically coupled state, depending on the relative energetic ordering of the three possible magnetic configurations (ferromagnetic, antiferromagnetic and non-spin-polarized).[25] In order to check this assumption, J has been calculated for double supercells of various length $2nd_0$ containing two monovacancies at nd_0 distance, retrieving the expected damped oscillatory behavior (Fig. 2, triangular marks). Indeed, the one-monovacancy supercells having zero magnetization (zero value in Fig. 2 square marks) correspond to a two-monovacancy system where the antiferromagnetic coupling is favored ($J>0$ in Fig. 2 triangular marks).

Even though the indirect coupling is quite weak (J is of the order of a few meV), it clearly affects the PBC computation of the magnetic properties of defected CNTs. Consequently, to accurately describe the local magnetic properties of isolated vacancies, an open system with a single magnetic impurity has to be considered. The defected CNTs are thus modeled as two semi-infinite sections of nanotube and a central region (or *core*) containing a single defect site, as described in.[26] Using this approach, the magnetization of the tilted monovacancy has always been found to be finite and converges for a core region consisting of $1\times1\times15$ cells as shown in Fig. 2, circular marks.[27]

It can further be noticed that both the open system and the PBC approaches can be considered as first approximations to "real" CNTs with low or high densities of defects, respectively. On one hand, the open system scheme can approximate the experimental case of low densities of vacancies only when the separation between defects is larger than the interaction range of the indirect exchange coupling. This interaction is found to depend on the location of the magnetic impurity on the hexagonal network of the host CNT (Ref. 24) and can vary from about 3 to 10 nm. Consequently, the open system approach can model a "real" defected CNT where vacancies are more than ~3–10 nm apart. On the other hand, the PBC approach presents some intrinsic limitations in describing the opposite limit of high density of vacancies in CNTs, as recently illustrated for magnetic impurities in graphene.[25] Indeed, a PBC calculation with one defect per unit cell always forces the periodically repeated magnetic impurities to be in the same spin state (either non-spin-polarized or ferromagnetically coupled). The antiferromagnetic or non-collinear spin polarization of the magnetic impurities cannot be described within such approach. Besides, the periodicity of a PBC calculation is an ideal model which imposes spurious interactions that are not present in the real system where the distribution of defects is random. Consequently, the PBC technique cannot model "real" CNTs with high density of defects, unless the defects are equally and ideally spaced and presents either no-coupling (no spin-polarization) or a ferromagnetic one.

C. Spin-polarized quantum electron transport

Having clarified the way to address the problem of studying the magnetic properties of a single defect site in CNTs, the open system scheme with a core of $1\times1\times15$ cells and the DZP basis set is used to predict both the magnetization and the spin polarized conductance of the defected tubes (see Fig. 3). From these calculations, it can be seen that the open-system scheme allows one to recover the expected magnetic behavior of mono-, di-, and trivacancies. In addition, our results definitely assess that the magnetization of defected CNTs can be ascribed to the presence of unsaturated carbon atoms, in agreement with a naive picture of a dangling bond.

The spin-polarized electron transport calculations are performed within the NEGF formalism, using the open-system scheme where the left and right semi-infinite sections of pristine (5,5) CNT have the role of contact electrodes (leads) and the scattering region consists of the $1\times1\times15$ core cells embedded by three leadlike cells on each side. In the absence of an external potential and considering a strong coupling between the scattering region and the leads, the NEGF formalism reduces to the Landauer-Büttiker description for equilibrium transport,[28] where the electron conductance $G(E)$ and the transmission function $T(E)$ at a given energy E are related by $G(E)=T(E)G_0$, where $G_0=2e^2/h$ is the quantum of conductance. Within such an approach, the ballistic conductance of a perfect system is proportional to the number of conducting channels, that is, the number of bands at a given

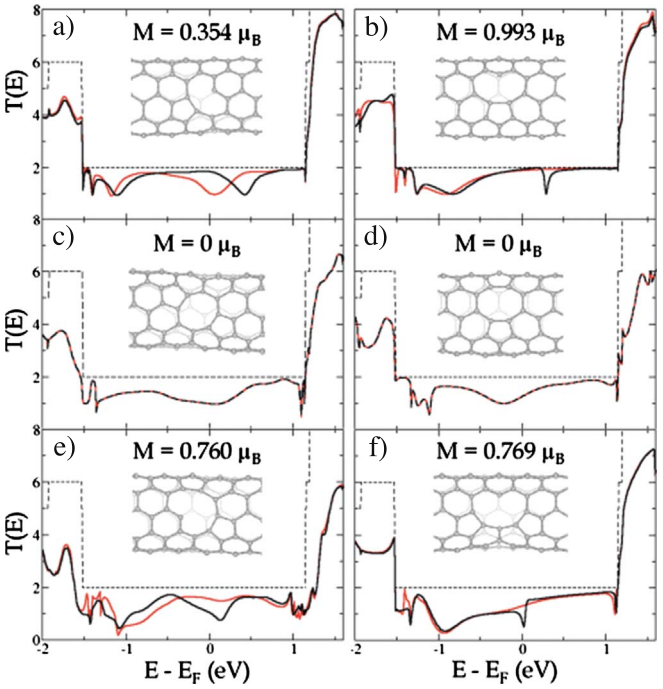

FIG. 3. (Color online) From top to bottom, spin-polarized electronic conductances of the (5,5) CNT with mono-, di-, and trivacancy in the tilted (left column) and parallel (right column) configurations. The corresponding optimized atomic structures are illustrated in insets. The magnetization, calculated within the open-system scheme, is also reported. The conductance of the pristine (5,5) tube is indicated by a dashed line. Red and black curves correspond to majority and minority spin channels, respectively.

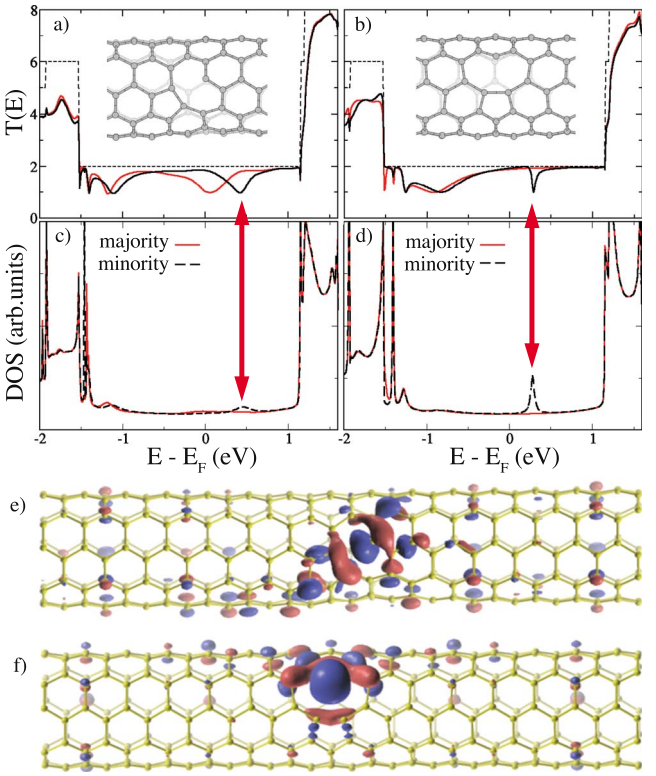

FIG. 4. (Color online) DoS calculated within the NEFG formalism for the (5,5) CNT containing a monovacancy reconstructed in its most stable (c) and next stable (d) configurations. The DoS allows to identify the degree of localization of the dips in the transmission curve (indicated by arrows), also reported in the figure [(a) and (b)] to facilitate the comparison. Red and black curves correspond to majority and minority spin channels, respectively. Wave functions illustrate the degree of localization of these electronic states. The tilted vacancy induces a more extended state (e) than the parallel one (f).

energy E. Indeed, the band structure of armchair CNTs is characterized by two energy bands crossing in the vicinity of the Fermi energy (E_F), inducing a conductance of $2G_0$ in the corresponding energy window (Fig. 3, dashed line). However, the conductance of an imperfect system is lowered, since the defect acts as a scattering center,[29,30] resulting in some dips in the conductance curve, as already observed for the tilted monovacancy in non-spin-polarized[3,30,31] and spin-polarized calculations.[15]

The conductance curves (Fig. 3, full lines) reveals that a carbon nanotube containing a mono- or trivacancy may act as a spin filter within some specific energy windows. For instance, the conductance at E_F of the tilted reconstruction of the monovacancy [Fig. 3(a)] drops from $2G_0$ to G_0 for one spin channel (majority spin carriers) while the minority spin conductance is almost unaffected. Consequently, at E_F, half of electrons with majority spin orientation will be filtered out while minority electrons will be almost fully transmitted. The situation is reversed at 0.4 eV: majority electrons are almost fully transmitted while half of minority electrons are reflected. A similar behavior is predicted for the parallel monovacancy [Fig. 3(b)] and for the tilted [Fig. 3(e)] and parallel trivacancy (Fig. 3(f)).

The conductance dips correspond to states which are quasilocalized [wide dips, Fig. 3(a) and Fig. 3(e)] or strongly localized [sharp dips, Fig. 3(b) and Fig. 3(f)] on the under-coordinated carbon, as can be seen from the height of the peaks of the density of states [density of states (DoS), Fig. 4(c) and Fig. 4(d), respectively] computed from the Green's function of the open system. The information on the degree of localization of the states on the defect site obtained from the conductance and the DoS computed within the open system scheme helps in better understanding why the range of the exchange coupling is so long and affects the magnetization computed in PBC. Indeed for the mono- and trivacancy in the parallel configuration, electronic states are more localized on the defect site [Fig. 4(f)] and, hence, little coupling between adjacent cells is found within the PBC scheme. On the other hand, for the mono- and trivacancy in the tilted configuration, the electronic states localized on the defect sites are also extended on the whole cell [Fig. 4(e)], resulting in a strong coupling of the magnetic impurities. The spatial extension of the quasilocalized states is inversely proportional to the tube radius R and the indirect coupling will have the same $1/R$ dependence.[24] For this reason, oscillations in the magnetic moment are less pronounced in the parallel case and in the graphene case.

At last, a comparison with previous spin-polarized calculations[15] of defected CNTs is called for. Indeed, this work predicts the (10,10) CNT containing a reconstructed monovacancy to be nonmagnetic, while our calculations sug-

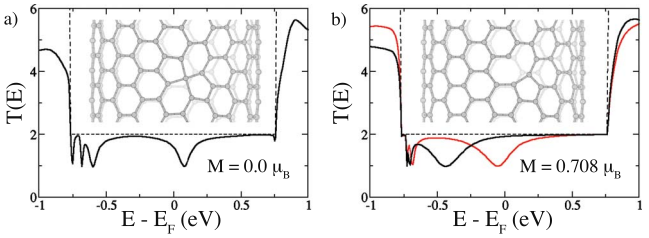

FIG. 5. (Color online) Quantum electron conductance and total magnetic moment for the (10,10) CNT containing a reconstructed monovacancy relaxed using the SZ (a) and the DZ (b) quality basis set. The magnetic moment is calculated using the open-system scheme. Red and black curves in (b) correspond to majority and minority spin channels, respectively.

gest that any vacancy containing carbon atoms with unsaturated bonds should behave as a magnetic impurity, resulting in a finite magnetization of the host tube. To clarify this apparent discrepancy, the (10,10) CNT with monovacancy has been studied using a single-ζ quality basis set (SZ), analogously to Ref. 15. When this basis set is used, the monovacancy reconstructs into a structure without dangling bonds [inset of Fig. 5(a)] which has been already observed to be a metastable configuration by using molecular dynamics.[21] Such metastable configuration is lower in energy by 0.153 eV with respect to the tilted configuration where the C_D atom is twofold coordinated [using the same labeling as for the (5,5) nanotube in Fig. 1(a)] Since this metastable reconstruction has no dangling bonds, no magnetism will result for this defect, leading the transmission curve to be non-spin-polarized, as illustrated in Fig. 5(a).

On the other hand, if a DZ-quality basis set is employed the correct energetic ordering is restored, with the tilted configuration lower in energy by 0.351 eV with respect to the mestastable one. In this case, the C_D atom has an unsaturated bond and the system is magnetic with a total magnetic moment of 0.708 μ_B and a spin-polarized conductance [Fig. 5(b)], consistently with the results obtained for the (5,5) defected tube.

IV. CONCLUSION

In conclusion, the magnetism and the spin polarized conductances of metallic CNTs containing vacancies have been investigated using first-principles and NEGF techniques. In particular, the debate on the PBC calculated values of the magnetization has been explained in terms of a long ranged interaction between the magnetic impurities. Besides, the problem of evaluating the local magnetic properties has been addressed by using an open system model containing a single magnetic impurity. Within this framework, it has been found that carbon atoms with unsaturated bonds always play the role of magnetic impurities in the host tube, hence establishing a connection between observed magnetism and creation of vacancies in carbon nanostructures and, finally, suggesting the possibility of exploiting the controlled introduction of defects in CNTs for spintronic applications.

ACKNOWLEDGMENTS

J.-C.C. acknowledges financial support from the F.R.S.-FNRS of Belgium. Parts of this work are directly connected to the Nano2Hybrids project (Grant No. EC-STREP-033311), to the Belgian Program on Interuniversity Attraction Poles (PAI6) on "Quantum Effects in Clusters and Nanowires," to the ARC "Hybrid metal/organic nanosystems" sponsored by the Communauté Française de Belgique. Computational resources have been provided by the Université catholique de Louvain: all the numerical simulations have been performed on the LEMAITRE and GREEN computers of the CISM.

[1] S. Iijima, Nature (London) **354**, 56 (1991).
[2] J.-C. Charlier, X. Blase, and S. Roche, Rev. Mod. Phys. **79**, 677 (2007).
[3] S. M.-M. Dubois, Z. Zanolli, X. Declerck, and J.-C. Charlier, Eur. Phys. J. B **72**, 1 (2009).
[4] P. Avouris, Z. Chen, and V. Perebeinos, Nat. Nanotechnol. **2**, 605 (2007).
[5] S. Sahoo, T. Kontos, J. Furer, C. Hoffmann, M. Gräber, A. Cottet, and C. Schönenberger, Nat. Phys. **1**, 99 (2005); L. E. Hueso, J. M. Pruneda, V. Ferrari, G. Burnell, J. P. Valdés-Herrera, B. D. Simons, P. B. Littlewood, E. Artacho, A. Fert, and N. D. Mathur, Nature (London) **445**, 410 (2007); J. R. Hauptmann, J. Paaske, and P. E. Lindelof, Nat. Phys. **4**, 373 (2008).
[6] K. Tsukagoshi, B. W. Alphenaar, and H. Ago, Nature (London) **401**, 572 (1999).
[7] W. Liang, M. Bockrath, D. Bozovic, J. H. Hafner, M. Tinkham, and H. Park, Nature (London) **411**, 665 (2001); S. Frank, P. Poncharal, Z. L. Wang, and W. A. de Heer, Science **280**, 1744 (1998); A. Bachtold, C. Strunk, J.-P. Salvetat, J.-M. Bonard, L. Forró, T. Nussbaumer, and C. Schönenberger, Nature (London) **397**, 673 (1999); A. Javey, J. Guo, Q. Wang, M. Lundstrom, and H. J. Dai, *ibid.* **424**, 654 (2003); J. Y. Park, S. Rosenblatt, Y. Yaish, V. Sazonova, H. Ustünel, S. Braig, T. A. Arias, P. W. Brouwer, and P. L. McEuen, Nano Lett. **4**, 517 (2004).
[8] K. Hata, D. N. Futaba, K. Mizuno, T. Namai, M. Yumura, and S. Iijima, Science **306**, 1362 (2004).
[9] A. Hashimoto, K. Suenaga, A. Gloter, K. Urita, S. Iijima, Nature **430**, 870 (2004); Y. Fan, B. R. Goldsmith, and P. G. Collins, Nature Mater. **4**, 906 (2005); K. Suenaga, H. Wakabayashi, M. Koshino, Y. Sato, K. Urita, and S. Iijima, Nat. Nanotechnol. **2**, 358 (2007).
[10] C. Gomez-Navarro, P. J. De Pablo, J. Gómez-Herrero, B. Biel, F. J. Garcia-Vidal, A. Rubio, and F. Flores, Nature Mater. **4**, 534 (2005).
[11] P. Esquinazi, D. Spemann, R. Höhne, A. Setzer, K.-H. Han, and T. Butz, Phys. Rev. Lett. **91**, 227201 (2003); S. Talapatra, P. G. Ganesan, T. Kim, R. Vajtai, M. Huang, M. Shima, G. Ramanath, D. Srivastava, S. C. Deevi, and P. M. Ajayan, *ibid.* **95**, 097201 (2005); Y. Shibayama, H. Sato, T. Enoki, and M. Endo, *ibid.* **84**, 1744 (2000); P. O. Lehtinen, A. S. Foster, Y. Ma, A. V. Krash-

eninnikov, and R. M. Nieminen, *ibid.* **93**, 187202 (2004); P. O. Lehtinen, A. S. Foster, A. Ayuela, T. T. Vehviläinen, and R. M. Nieminen, Phys. Rev. B **69**, 155422 (2004).

[12] Y. Ma, P. O. Lehtinen, A. S. Foster, and R. M. Nieminen, New J. Phys. **6**, 68 (2004).

[13] S. Berber and A. Oshiyama, Physica B **376-377**, 272 (2006).

[14] S. Berber and A. Oshiyama, Phys. Rev. B **77**, 165405 (2008).

[15] Y.-W. Son, M. L. Cohen, and S. G. Louie, Nano Lett. **7**, 3518 (2007).

[16] For instance, the magnetization of the lowest-energy reconstruction of the (5,5) tube containing a monovacancy is 0.6 μ_B for the $1\times1\times5$ supercell and zero for $1\times1\times n$ supercells with n larger than 5 in Ref. 12 and it is less the 1 μ_B for the $1\times1\times12$ supercell in Ref. 13.

[17] J. M. Soler, E. Artacho, J. Gale, D. A. Garcia, J. Junquera, P. Ordejón, and D. Sánchez-Portal, J. Phys.: Condens. Matter **14**, 2745 (2002).

[18] A. R. Rocha, V. M. Garcia-Suárez, S. W. Bailey, C. J. Lambert, J. Ferrer, and S. Sanvito, Phys. Rev. B **73**, 085414 (2006).

[19] N. Troullier and J. L. Martins, Phys. Rev. B **43**, 1993 (1991).

[20] The convergence and the accuracy of the DZP basis set used to describe the magnetic properties of defected CNTs have been checked using the ABINIT plane-wave code [X. Gonze, *et al.*, Comput. Mater. Sci. **25**, 478 (2002)].

[21] P. M. Ajayan, V. Ravikumar, and J.-C. Charlier, Phys. Rev. Lett. **81**, 1437 (1998).

[22] H. Amara, S. Latil, V. Meunier, P. Lambin, and J.-C. Charlier, Phys. Rev. B **76**, 115423 (2007).

[23] J. Kotakoski, A. V. Krasheninnikov, and K. Nordlund, Phys. Rev. B **74**, 245420 (2006).

[24] D. F. Kirwan, C. G. Rocha, A. T. Costa, and M. S. Ferreira, Phys. Rev. B **77**, 085432 (2008), and references therein.

[25] P. Venezuela, R. B. Muniz, A. T. Costa, D. M. Edwards, S. R. Power, and M. S. Ferreira, Phys. Rev. B **80**, 241413(R) (2009).

[26] Z. Zanolli and J.-C. Charlier, Phys. Rev. B **80**, 155447 (2009).

[27] Being interested in the trend of the total magnetic moment with increasing cell size, the convergence study of the magnetic moment for the open system has been performed using a double-ζ (DZ) quality basis set, due to the high computational cost of the DZP calculations. However, it has been found that for the $1\times1\times7$ and the $1\times1\times15$ core cells the magnetizations calculated using the DZ and the DZP basis differ less than 0.06 μ_B. The tilted trivacancy has also been studied as an open system, finding convergence of the total magnetic moment for the $1\times1\times15$ core cell.

[28] M. Büttiker, Y. Imry, R. Landauer, and S. Pinhas, Phys. Rev. B **31**, 6207 (1985).

[29] L. Chico, L. X. Benedict, S. G. Louie, and M. L. Cohen, Phys. Rev. B **54**, 2600 (1996).

[30] H. J. Choi, J. Ihm, S. G. Louie, and M. L. Cohen, Phys. Rev. Lett. **84**, 2917 (2000).

[31] A. R. Rocha, J. E. Padilha, A. Fazzio, and A. J. R. da Silva, Phys. Rev. B **77**, 153406 (2008).